Journal of Radiation Research and Applied Sciences 17 (2024) 101196

Contents lists available at ScienceDirect

Journal of Radiation Research and Applied Sciences

journal homepage: www.journals.elsevier.com/journal-of-radiation-research-and-applied-sciences

Numerical solutions for unsteady laminar boundary layer flow and heat transfer over a horizontal sheet with radiation and nonuniform heat Source/Sink

Machindranath Diwate [a,b], Jagadish V. Tawade [b], Pradeep G. Janthe [b], Mubariz Garayev [c], Mohammed El-Meligy [d,e], Nitiraj Kulkarni [b], Manish Gupta [f], M. Ijaz Khan [g,*]

[a] Department of Mathematics, Sinhgad Institute of Technology and Science, Narhe Pune, 411041, India
[b] Department of Mathematics, Vishwakarma University, Pune, 411048, India
[c] Department of Mathematics, College of Science, King Saud University, P.O Box 2455, Riyadh, Saudi Arabia
[d] Jadara University Research Center, Jadara University, PO Box 733, Irbid, Jordan
[e] Applied Science Research Center, Applied Science Private University, Amman, Jordan
[f] Division of Research and Development, Lovely Professional University, Phagwara, India
[g] Department of Mathematics and Statistics, Riphah International University I-14, Islamabad 44000, Pakistan

A R T I C L E I N F O

Keywords:
Unsteady laminar boundary layer
Heat transfer
Magnetic field
Radiation
Nonuniform heat source
Fluid dynamics
Thermal management
Numerical analysis

A B S T R A C T

This paper investigates the unsteady laminar boundary layer flow and heat transfer over a horizontal sheet subjected to radiation and a nonuniform heat source/sink. The governing partial differential equations are transformed into ordinary differential equations using similarity transformations and solved via the bvp4c numerical method. The key findings indicate that increasing the unsteadiness parameter leads to a reduction in both velocity profiles and heat flux, while higher values of the Prandtl number reduce thermal boundary layer thickness. In contrast, the radiation and magnetic parameters enhance the temperature profile within the boundary layer. The study offers new insights into the effects of flow parameters on boundary layer behaviour, validated through table and graphical comparisons with existing literature. These findings provide practical approaches for optimizing heat transfer systems in engineering applications.

1. Introduction

Heat transfer and fluid flow in boundary layers have a wide range of applications in engineering and industrial processes, from microelectronics cooling to energy-efficient system designs. Understanding the behaviour of heat transfer in laminar boundary layers is crucial for optimizing these processes, particularly when dealing with unsteady conditions. The study of boundary layers on stretching surfaces has become increasingly important in recent years due to its relevance to industries such as materials processing, electronics, and even biomedical devices.

In many real-world systems, heat sources and sinks are not uniformly distributed. Nonuniform heat generation or absorption can occur due to spatial variations in material properties or the external environment. Similarly, thermal radiation plays a vital role in processes where high temperatures are involved, significantly impacting heat transfer rates. Despite extensive research into steady-state conditions, less attention has been given to unsteady laminar boundary layer flows with nonuniform heat sources and radiation effects, which more accurately reflect many practical scenarios.

While considerable research has been conducted on boundary layer flows and heat transfer, most studies have focused on steady-state conditions or specific cases, such as uniform heat sources and the absence of radiation. This study, however, goes beyond these limitations by investigating unsteady laminar boundary layer flow under the influence of both a nonuniform heat source/sink and thermal radiation, providing a more holistic view of these interactions in dynamic conditions. The work of Sakiadis (Sakiadis, 1961) introduced the fundamental boundary layer equations for continuous surfaces, which have become essential for understanding flow behaviour in many contexts. This foundational research is crucial for studies involving unsteady laminar boundary layer flow, such as the present investigation into heat transfer over a

* Corresponding author.
E-mail address: scientificresearchglobe@gmail.com (M.I. Khan).

https://doi.org/10.1016/j.jrras.2024.101196
Received 10 September 2024; Received in revised form 28 October 2024; Accepted 8 November 2024

horizontal sheet with radiation and non-uniform heat sources. Sakiadis (Sikiadis, 1961) extended his work on boundary layer behaviour by focusing on the effects of surface stretching. His findings are directly relevant to the current study, as they provide a deeper understanding of how stretching surfaces influence boundary layer flow and heat transfer, particularly in unsteady flow conditions. Crane (Crane, 1970) provided an exact solution for flow past a stretching plate, offering valuable theoretical insights for analyzing boundary layer flow over stretching surfaces. His work supports the present study's investigation into the dynamics of flow and heat transfer on a horizontally stretching sheet. The study by Tsai et al. (Tsai et al., 2008) examined flow and heat transfer over an unsteady stretching surface with non-uniform heat sources, which aligns closely with the present research. Their work provides insights into how non-uniform heat sources influence the thermal behaviour of boundary layers, a key aspect of the current study. Abel et al. (Abel, Tawade, & Nandeppanavar, 2009) explored the effects of magnetic fields and non-uniform heat sources on MHD heat transfer over an unsteady stretching surface. Their findings are highly relevant to this study's focus on the role of magnetic fields in enhancing temperature profiles within the boundary layer. In another paper, Abel et al. (Abel, Mahesha, & Tawade, 2009) investigated viscous dissipation and the influence of external magnetic fields on heat transfer. This research offers valuable context for understanding how magnetic parameters and viscous effects contribute to the temperature distribution in boundary layer flows, which is also examined in this study.

Recent advances by Nasir et al., and other researchers (Li et al., 2021; Nasir & Berrouk, 2024; Nasir et al., 2022, 2023a, 2023b, 2024; Qian et al., 2022; Sulochana et al., 2024; Teja et al., 2024; Zhao et al., 2021), have introduced the analysis of hybrid nanofluids, radiation effects, renewable and sustainable energy aspects and entropy generation in magnetohydrodynamic (MHD) flows. Their studies highlight nanofluids' enhanced heat transfer capabilities and the significant role of radiation and magnetic fields, all aligning with the current study's focus on optimizing heat transfer in boundary layers with non-uniform heat sources and sinks. Salahuddin et al. (Salahuddin, 2023) provide a thorough exploration of numerical techniques in MATLAB, essential for solving partial differential equations (PDEs) that describe boundary layer behavior. Their computational framework, applied to fluid dynamics, is directly applicable to the bvp4c method you are using to solve the transformed differential equations in your study. Furthermore, Awais et al., and other analysts (Awais et al., 2023, 2024; Awais and Salahuddin, 2023, 2024; Hamid et al., 2021) expands on the role of viscous dissipation, magnetic fields, and energy dissipation in non-Newtonian fluids, examining how these factors affect the heat transfer process in boundary layers. These studies are particularly useful for understanding how variable thermophysical properties, such as viscosity, affect heat transfer rates and flow behaviour in the presence of magnetic fields, which directly supports the analysis of MHD flow in your research. Further Salahuddin et al. (Salahuddin & Awais, 2023; Salahuddin et al., 2021a, 2021b, 2023) focuses on advanced models like the Cattaneo-Christov heat and mass flux theory for complex fluid flows. These models introduce mechanisms for dealing with transient and stratified boundary layers, enhancing the understanding of non-uniform heat transfer, which is central to your study. The combination of numerical methods and the examination of heat and mass transfer in dissipative fluids offers valuable insights into the complex dynamics involved in boundary layer flows under unsteady conditions. Sarfraz et al. (Sarfraz et al., 2023; Sarfraz & Khan, 2022) explore hybrid nanofluid flow over a shrinking surface, providing multiple solutions for optimizing heat transfer in radiative mixed convection scenarios.

Wang (Wang, 2006) provides analytic solutions for liquid film flow on an unsteady stretching surface, offering key insights into fluid dynamics and heat transfer in such systems. Bilal et al. (Bilal et al., 2023) develop analytic similarity solutions for unsteady laminar boundary layer flow and heat transfer under radiation, advancing the understanding of how radiation impacts boundary layer behaviour.

Zhang et al. (Zhang et al., 2023) investigate the management of energy in renewable networks under uncertainty. Their method optimizes the system's reliability, which parallels the need to understand complex, dynamic conditions in fluid and thermal systems. Khalafian et al. (Khalafian et al., 2024) focus on compressed air energy storage in off-grid renewable systems. This research highlights the importance of flexible storage solutions in energy systems, much like how heat sources and sinks affect boundary layer behavior in fluid systems. Liang and Pirouzi (Liang & Pirouzi, 2024) explore economic management of smart distribution networks integrating hydrogen storage. Their approach to managing fluctuating energy flows mirrors the challenges addressed in this manuscript, particularly the influence of varying heat sources on boundary layer thickness and heat flux. Kazemi et al. (Kazemi et al., 2022) propose strategies for energy storage participation in day-ahead markets. Their work on coordinated management strategies aligns with the control of parameters such as unsteadiness and radiation in fluid systems for optimized heat transfer. Pirouzi (Pirouzi, 2023) presents a virtual power plant model dealing with network constraints, emphasizing efficient energy distribution. This approach relates to the study's focus on optimizing boundary layer behavior through careful manipulation of magnetic and radiation parameters. Norouzi et al. (Norouzi, Aghaei, Niknam, et al., 2022) and (Norouzi, Aghaei, Pirouzi, et al., 2022) focus on flexible energy pricing and microgrid stability, addressing system uncertainties. Their contributions highlight how incorporating flexibility into systems, similar to the flexibility in managing boundary conditions in this manuscript, is key to achieving optimal performance in dynamic environments. Muhammad et al. (Muhammad et al., 2024; Sarfraz & Khan, 2024) conduct a statistical and numerical analysis of electrically conducting hybrid nanomaterials near the stagnation region, focusing on heat transfer and flow behavior in critical areas.

This study addresses a gap in the existing literature by investigating the unsteady laminar boundary layer flow and heat transfer over a horizontal sheet with the combined effects of radiation and non-uniform heat sources/sinks. Previous research has extensively analysed nanofluids, magnetic fields, radiation, and numerical methods, all of which contribute to a deeper understanding of complex fluid dynamics. These studies provided essential insights into heat transfer mechanisms, MHD flows, and computational techniques, which align with and support the findings of this research.

We extend these contributions by using the bvp4c numerical method to solve the transformed boundary layer equations, offering a novel approach to the combined effects of radiation, magnetic fields, and non-uniform heat sources. This research offers practical insights for optimizing thermal management systems in engineering applications, including cooling in microelectronics, heat transfer in manufacturing, and energy-efficient system design.

2. Mathematical formulation

Consider a thin elastic liquid film of uniform thickness $h(t)$ resting on a horizontal stretching sheet (Fig. 1). The x-axis aligns with the direction of the sheet's motion, while the y-axis is perpendicular to it. The fluid under consideration is non-volatile, viscous, incompressible, and subject to unsteady two-dimensional flow on a thin horizontal surface. The sheet experiences stretching due to two equal and opposite forces along the x-axis, with a velocity U defined in Eq. (7), and is exposed to an external transverse magnetic field of strength B. We neglect the effect of latent heat due to evaporation, assuming the liquid to be non-volatile. Additionally, we assume the viscosity of the fluid remains constant throughout and is unaffected by temperature changes. Although buoyancy effects are negligible due to the thinness of the liquid film, it is thick enough to avoid the influence of intermolecular forces. Both velocity and temperature vary with time t and along the x-coordinate. The governing equations of continuity, momentum, and energy are as below (See refs (Wang, 2006). and (Bilal et al., 2023))

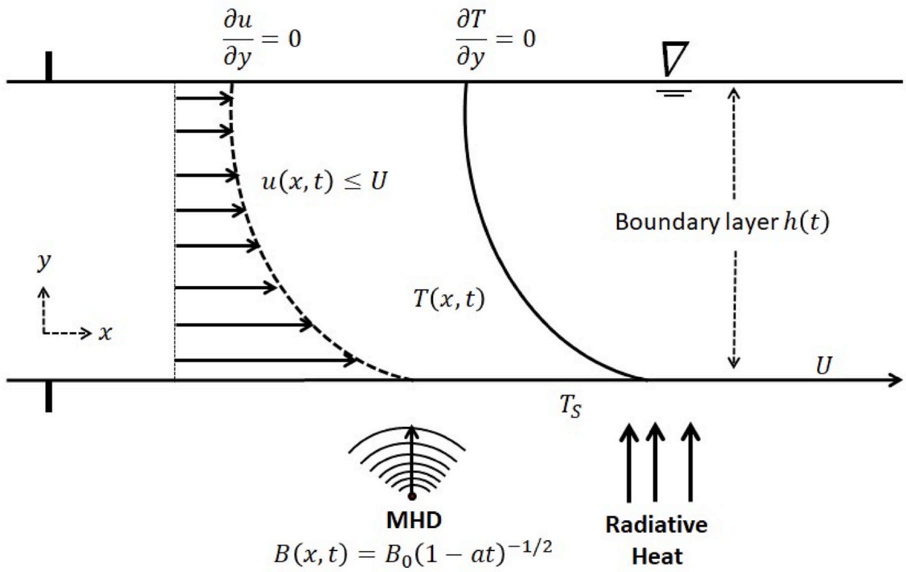

Fig. 1. Schematic diagram for velocity and temperature distribution.

$$\frac{\partial u}{\partial x} + \frac{\partial v}{\partial y} = 0, \tag{1}$$

$$\frac{\partial u}{\partial t} + u\frac{\partial u}{\partial x} + v\frac{\partial u}{\partial y} - \frac{\rho}{\mu}\frac{\partial^2 u}{\partial y^2} = 0, \tag{2}$$

$$\frac{\partial T}{\partial t} + u\frac{\partial T}{\partial x} + v\frac{\partial T}{\partial y} = \frac{k}{\rho C_p}\frac{\partial^2 T}{\partial y^2} - \frac{1}{\rho C_p}\frac{\partial q^r}{\partial y} + \frac{\mu}{\rho C_p}\left(\frac{\partial u}{\partial y}\right)^2 + \frac{\sigma B^2}{\rho C_p}u^2 + \frac{q'''}{\rho C_p}, \tag{3}$$

Subject to,

$$u = U(x,t), v = 0, T = T_S(x,t), at\, y = 0$$

$$u_y = T_y = 0, v = h_t, at\, y = h(t) \tag{4}$$

Where u and v are the velocities in x and y-directions, respectively. μ is the dynamic viscosity, ρ is the density of flowing fluid, T is the temperature, k is the thermal conductivity, C_p is the specific heat at constant pressure, q^r is heat flux due to radiation which according to Rosseland approximation (See Ref (Bilal et al., 2023).) is written as,

$$q^r = -\frac{4\sigma}{3k^*}\left(\frac{\partial T^4}{\partial y}\right). \tag{5}$$

Further, U is the surface velocity, $T(x,t)$ is the surface temperature and h is the thickness of boundary layer (liquid film). Where σ and k^* are the Stefan-Boltzmann constant and mean absorption coefficient respectively. Temperature T in (5) can be assumed as a linear function for the small variations in temperature and it can be expressed after neglecting higher-order terms in the Taylor's expansion as,

$$T^4 \cong 4T_0^3T - 3T_0^4. \tag{6}$$

2.1. Existing similarity transformations

Wang (Wang, 2006) and Bilal et al. (Bilal et al., 2023) provides similarity transformations that are used by M. Subhas Abel (Abel, Tawade, & Nandeppanavar, 2009) to study a similar type of problem. At $y = 0$ the flow velocity in x-direction and surface temperature are considered as,

$$U = \frac{bx}{(1-at)}, \tag{7}$$

$$T_S = T_0 - T_{ref}\left(\frac{dx^2\rho}{2\mu(1-at)^{3/2}}\right). \tag{8}$$

In (7) and (8), a and b are positive constants with $(time^{-1})$ dimensions. T_{ref} is the reference temperature, T_o is the temperature at the origin of the slit and d is a constant. This special form of surface velocity (7) and temperature (8) allows us to create and implement the following transformations,

$$\eta = \frac{y}{\beta}\left(\frac{b\rho}{\mu(1-at)}\right)^{1/2}, \tag{9}$$

$$u = \frac{bx}{(1-at)}f'(\eta), \tag{10}$$

$$v = -\beta\left(\frac{\mu b}{\rho(1-at)}\right)^{\frac{1}{2}}f(\eta), \tag{11}$$

$$T = T_0 - T_{ref}\left(\frac{dx^2\rho}{2\mu(1-at)^{\frac{3}{2}}}\right)\theta(\eta), \tag{12}$$

Where η is the similarity variable, f is the stream function, θ is the dimensionless temperature, and β is the dimensionless film thickness which is unknown. By using the transformations (9) – (12) (*see Ref*. [30]), the continuity equation (1) is satisfied and this reduces the number of equations from three to two. The momentum equation (2) and the energy equation, by substituting mappings (9) – (12) and simplification using (6), transform to a third and a second order ODE, respectively, i.e., the system of PDEs (1) – (3) and the associated boundary conditions (4) thus are written as,

$$f''' + \lambda\left(ff'' - \frac{1}{2}S\eta f'' - (f')^2 - Sf'\right) = 0,$$

$$\frac{1}{Pr}\left(1 + \frac{4R}{3}\right)\theta'' + \lambda\left(f\theta' - 2f'\theta - \frac{1}{2}\eta S\theta' - \frac{3}{2}S\theta + M\,Ec\,f'^2 + \frac{1}{Pr}(A^*f' + B^*\theta)\right) + Ec\,f''^2 = 0, \tag{13}$$

and

$$f(0)=0, f'(0)=1, \theta(0)=1, f(1)=\frac{1}{2}S, f''(1)=0, \theta'(1)=0. \quad (14)$$

All the conditions on $f(\eta)$ and its derivatives that are given above are obtained using transformations (9) – (11) while all on $\theta(\eta)$ and its derivatives are obtained through (9) and (12). In the above system of ODEs $\lambda=\beta^2$ is the unknown dimensionless film thickness, $S=a/b$ denotes the dimensional unsteadiness parameter while $R=\frac{4\sigma T_0^3}{k^*}$ and $Pr=\frac{\mu C_p}{k}$ are radiation parameter and Prandtl number, respectively.

The applied transverse magnetic field (see (Abel, Tawade, & Nandeppanavar, 2009)) is assumed to be of variable kind and is chosen in its special form as

$$B(x,t)=\frac{B_0}{(1-at)^{1/2}},$$

The non-uniform heat source/sink (see (Abel, Tawade, & Nandeppanavar, 2009)) is modelled as

$$q'''=\frac{kU_w(x)}{x\nu}[A^*(T_s-T_0)f'+(T-T_0)B^*],$$

Where A^* and B^* are the coefficients of space and temperature dependent heat source/sink respectively. Here we make a note that the case $A^*>0, B^*>0$ corresponds to internal heat generation and that $A^*<0$, $B^*<0$ corresponds to internal heat absorption.

The magnetic field Parameter (see (Salahuddin, Awais, Khan, & Altanji, 2021), 25) is

$$M=\frac{\sigma B_0^2}{\rho a},$$

The Eckert number (see (Nasir et al., 2022)) is

$$Ec=\frac{U^2}{C_p(T_s-T_0)}.$$

The important physical parameters of flow and heat transfer are the skin friction and heat flux. Skin friction C_f and heat flux q^r can be written as,

$$C_f=2Re_x^{-\frac{1}{2}}\beta^{-1}f''(0) \quad (15)$$

$$q^r=-k\left(\frac{\partial T}{\partial y}\right)_{y=0} \quad (16)$$

Where shear stress τ_S and local Reynolds number Re_x is defined as

$$\tau_S=\mu\left(\frac{\partial u}{\partial y}\right)_{y=0} \quad (17)$$

$$Re_x=\frac{\rho u x}{\mu}. \quad (18)$$

In fluid flow and heat transfer, key parameters like the skin friction coefficient (C_f) and heat flux (q^r) are crucial for understanding system behaviour. The skin friction coefficient is a dimensionless measure of surface drag caused by viscous forces and is linked to the local Reynolds number (Re_x) and shear stress at the wall. Heat flux represents the rate of heat transfer across a surface, governed by the temperature gradient and the fluid's thermal conductivity (k). These parameters are essential for optimizing fluid and thermal system performance, energy efficiency, and material durability.

The solutions to the governing equations in this study will provide valuable insights into practical engineering applications. They will help optimize thermal management systems, such as cooling in microelectronics and engines, and are critical in material processing industries like polymer and glass manufacturing where precise control of heat transfer is essential. Additionally, these solutions can guide the design of more energy-efficient systems by improving the understanding of fluid dynamics and heat transfer by offering practical benefits beyond their mathematical significance.

3. Numerical approach

The bvp4c method is a MATLAB-based numerical solver used to solve boundary value problems for ordinary differential equations (ODEs). In this study it was used to obtain numerical solutions to the transformed boundary layer flow and heat transfer equations. This method is particularly well-suited for solving problems involving nonlinear and coupled ODEs with boundary conditions specified at two or more points.

It efficiently handles nonlinear systems, as in the case of the transformed boundary layer equations. Additionally, the adaptive mesh refinement technique used by bvp4c ensures accurate solutions even in regions with rapid changes, such as near the surface of the stretching sheet. The solver also allows for flexibility in handling the complex boundary conditions typical of boundary layer flow problems, making it a robust choice for this investigation. The method's accuracy and flexibility in solving nonlinear boundary value problems are key reasons for its selection in this study.

The model (13)–(14) consists of highly Coupled non-linear ODEs which are solved numerically. In present case we adopt the efficient bvp4c method to obtain the numerical solutions of (13)–(14). The ODEs (13)–(14) are reduced to simultaneous equations of first-order, as follows.

$$f=f_1 \quad (19)$$

$$f'=f_2 \quad (20)$$

$$f''=f_3, \quad (21)$$

$$f'''=-\lambda\left[f_1f_3-\left(\frac{1}{2}\right)S\eta f_3-f_2f_2-Sf_2\right], \quad (22)$$

$$\theta=f_4, \quad (23)$$

$$\theta'=f_5, \quad (24)$$

$$\theta''=\frac{-Pr}{\left(1+\frac{4R}{3}\right)}\left[\lambda\left(f_1f_5-2f_2f_4-\left(\frac{1}{2}\right)\eta Sf_5-Sf_4+MEcf_1{}^2+\frac{1}{Pr}(A^*f'+B^*\theta)\right)+Ecf''^2\right], \quad (25)$$

Corresponding boundary conditions are expressed as,

$$f_1(0)=0, f_2(0)=1, f_4(0)=1, f_1(1)=\frac{1}{2}S, f_3(1)=0, f_5(1)=0. \quad (26)$$

Table 1
Validation of Numerical solution by using *BVP4C*.

S	Wang (Wang, 2006)		Bilal et al. (Bilal et al., 2023)		Present Study	
	β	$-f''(0)$	β	$-f''(0)$	β	$-f''(0)$
1.0	1.54362	1.97238	1.54361606	1.97238487	1.543617	1.207259
1.2	1.127780	1.442631	1.12778094	1.44262519	1.127780	1.397506
1.4	0.821032	1.012784	0.82103222	1.01278017	0.821033	1.012780
1.6	0.576173	0.642397	0.57617302	0.64239699	0.576176	0.642382

Table 2
Validation of values of temperature profile $\theta(\beta)$ and wall temperature gradient $-\theta'(0)$.

Pr	Present Values		Wang (Wang, 2006)		
	$\theta(\beta)$	$-\theta'(0)$	$\theta(\beta)$	$-\theta'(0)$	$\frac{-\theta'(0)}{\beta}$
$\beta = 2.15199, S = 0.8$					
0.01	0.960438	0.042120	0.960480	0.090474	0.042042
0.1	0.692296	0.351920	0.692533	0.756162	0.351378
1	0.097825	1.671919	0.097884	3.595790	1.670913
2	0.024869	2.443914	0.024941	5.244150	2.436884
3	0.008324	3.034915	0.008785	6.514440	3.027170
$\beta = 1.127780, S = 1.2$					
0.01	0.982312	0.033515	0.982331	0.037734	0.033458
0.1	0.843485	0.305409	0.843622	0.343931	0.304962
1	0.286634	1.773772	0.286717	1.999590	1.773032
2	0.128174	2.638431	0.128124	2.975450	2.638324
3	0.067737	3.280329	0.067658	3.698830	3.279744

Note: Wang (Wang, 2006) has used different similarity transformation due to which the value of $-\theta(0)/\beta$ in his paper is the same as $-\theta'(0)$ of our results.

4. Result and discussion

The study of the effects of various parameters such as unsteadiness parameter, Prandtl number, radiation parameter, magnetic parameter, Eckert number, and heat source/sink parameter on boundary layer thickness, fluid velocity, skin friction, temperature, and heat flux are crucial for understanding and optimizing heat transfer and fluid flow in engineering applications. Here's a detailed discussion on the results and implications of each parameter variation.

Comparison of the numerical results from the present study with Wang (Wang, 2006) and Bilal et al. (Bilal et al., 2023) demonstrates that the values of β are consistently reproduced across the studies, confirming the reliability of the present numerical method (see Table 1). Table 2 depicts numerical results for temperature profile regarding rising values of Prandtl number. The slight variations in the skin friction coefficient $-f''(0)$ observed at certain values of S are within acceptable error margins and may be attributed to differences in the mathematical models and boundary conditions employed. Overall, the results show good agreement with the literature, validating the techniques used.

In the study, the following parameters are fixed at: $= 1.0$, $Pr = 1$ (Prandtl number), $R = 1$ (radiation parameter), $Ec = 1$ (Eckert number), $M = 1$ (magnetic parameter), $A^* = 0.5$ (space-dependent heat source), $B^* = 0$ 0.5 (temperature-dependent heat source), and $S = 2$ (unsteadiness parameter), (Refs. 29,30). The variations in any parameters are mentioned in the corresponding graphs.

Fig. 2 shows the variation of velocity distribution $f'(\eta)$ in the boundary layer with the unsteadiness parameter S over the stretching sheet. It is observed that the surface velocity $f'(1)$ approaches the velocity of boundary U as $S \rightarrow 2$. At $S = 2$ the flow velocity exactly matches the velocity of boundary (at $y = 0$) and flow synchronizes with the boundary and there is no boundary layer i.e., the relative fluid velocity is zero. We observe that higher unsteadiness creates a stronger synchronization between the flow and the boundary motion, thus reducing the relative motion (velocity) of the fluid away from the surface.

Fig. 3 provides a variation of temperature distribution $\theta(\eta)$ in the boundary layer with the unsteadiness parameter S in the stretching sheet. We notice that increasing S, the temperature within the boundary layer decreases. As higher values of S correspond to a more rapidly stretching surface, which in turn leads to faster cooling of the fluid. The thermal boundary layer becomes thinner as S increases, indicating that the unsteady motion assists more efficient heat transfer away from the

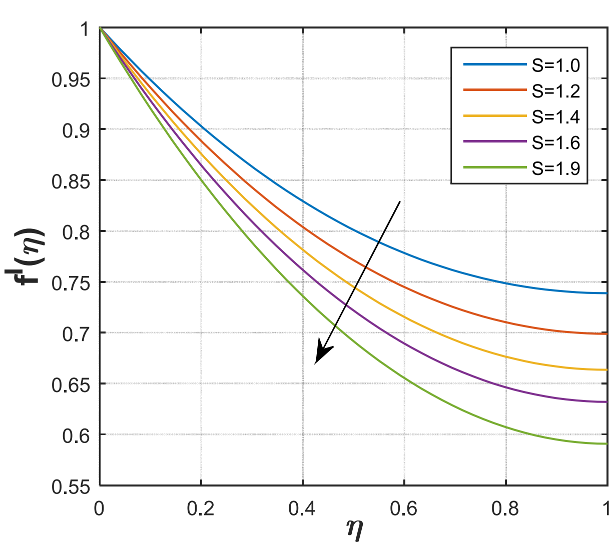

Fig. 2. Profile of velocity for S.

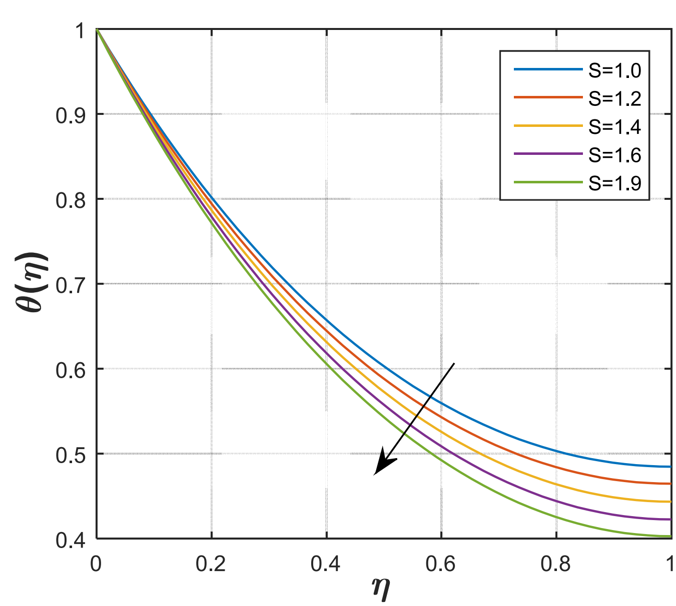

Fig. 3. Profile of temperature for S.

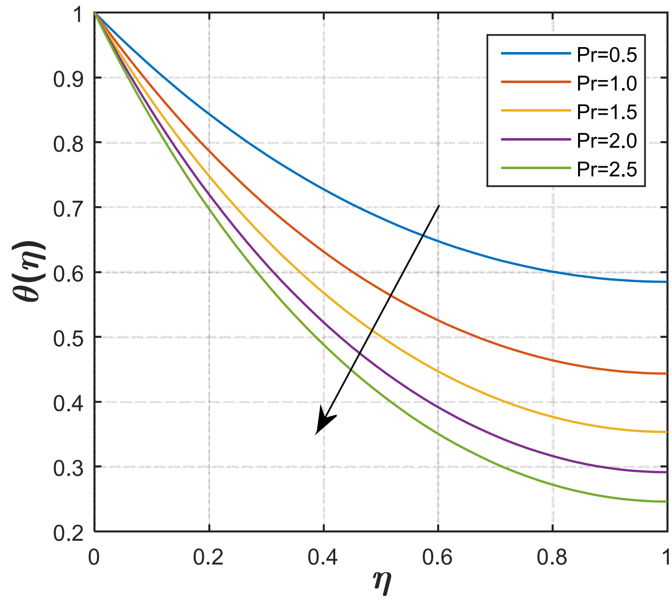

Fig. 4. Profile of temperature for ***Pr***.

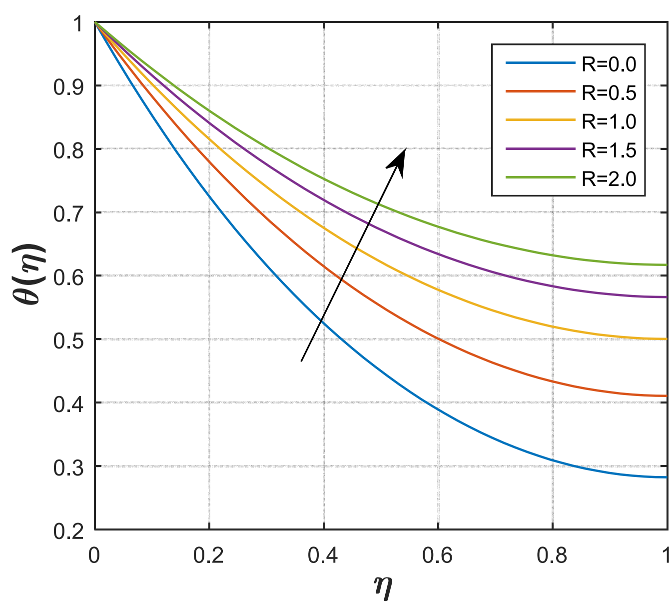

Fig. 5. Profile of temperature for R.

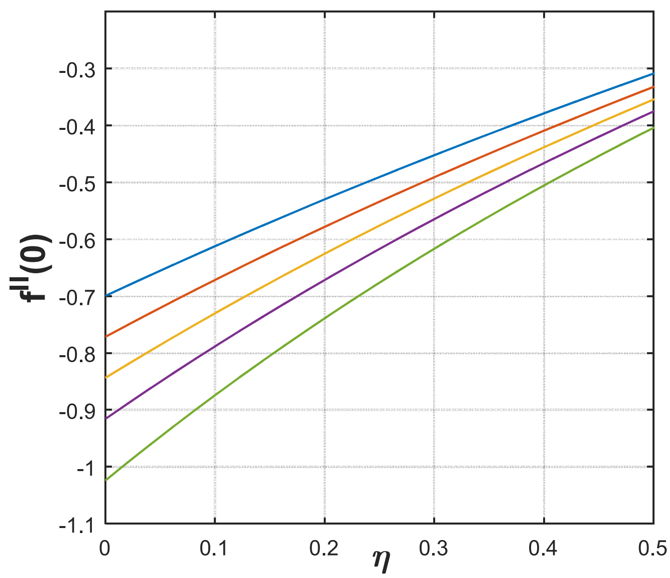

Fig. 6. Profile of skin friction for S.

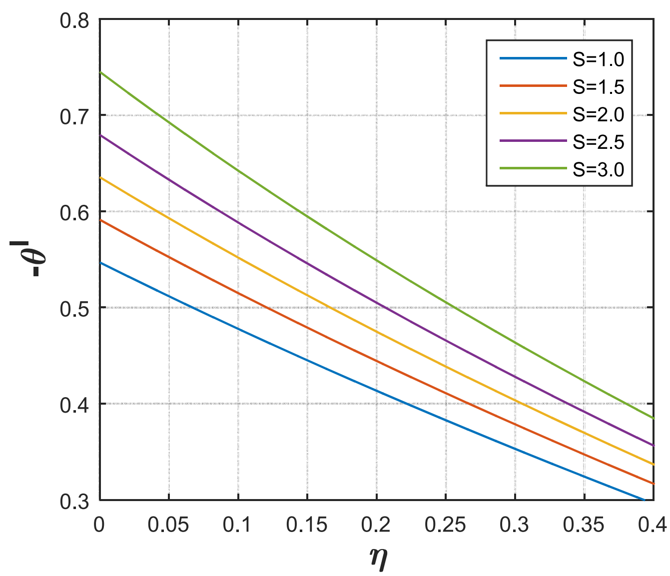

Fig. 7. Profile of nusselt number for S.

surface.

Fig. 4 highlight the effect of variation of temperature distribution $\theta(\eta)$ in the boundary layer with Prandtl number *Pr* in the stretching sheet. It is evident that the temperature distribution is a decreasing function of Prandtl number. This is because the thermal diffusivity of the fluid is decreases due to higher values of *Pr* which further leads to the reduction in the thermal boundary layer thickness. Due to the effect of the melting parameter, the thermal boundary layer thickness increases by an increasing value of *Pr* and also enhances the thermal boundary layer thickness.

Fig. 5 shows the variation of temperature distribution $\theta(\eta)$ in the boundary layer with Radiation Parameter *R* in the stretching sheet. As *R* increases, the temperature within the boundary layer rises, indicating that radiation enhances the energy transfer within the system. The radiation parameter represents the relative importance of thermal radiation compared to conduction, and as *R* increases, the contribution of radiation to the overall heat transfer becomes more significant. This leads to an increase in the fluid temperature near the surface. These results suggest that in systems where radiation plays a dominant role, increasing the radiation parameter can significantly impact the temperature distribution, enhancing thermal effects.

The results presented in Fig. 6 shows variation of skin friction coefficient $f''(0)$ in the boundary layer with the unsteadiness parameter *S* in the stretching sheet. As *S* increases, the skin friction coefficient decreases, indicating that the fluid's resistance to motion at the surface is reduced. This is consistent with the observed reduction in velocity profiles at higher values of *S*, where the fluid flow becomes more synchronized with the motion of the stretching sheet, resulting in lower frictional forces.

Fig. 7 demonstrates the effect of variation of heat flux $-\theta'(0)$ in the boundary layer with the unsteadiness parameter *S* in the stretching sheet. As *S* increases, the heat flux decreases, indicating that less heat is being transferred from the surface to the fluid. This is due to the reduced temperature difference between the surface and the fluid at higher values of *S*, which limits the amount of heat that can be conducted away from the surface. This suggests that in systems where high heat flux is

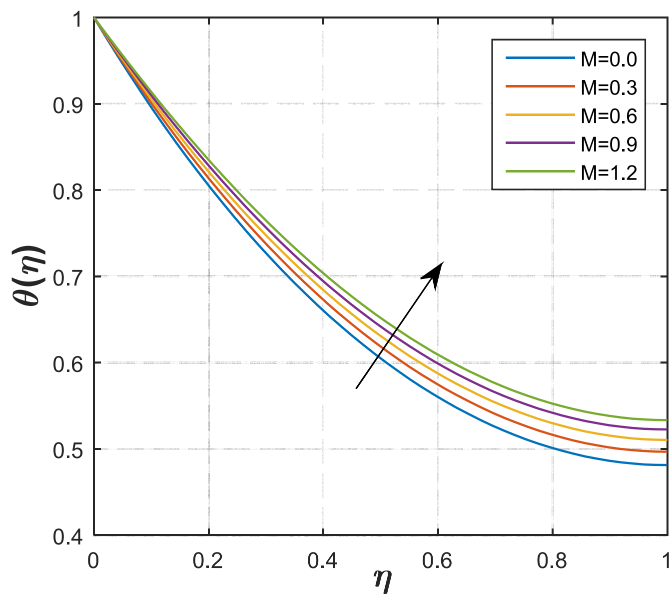

Fig. 8. Profile of temperature for M.

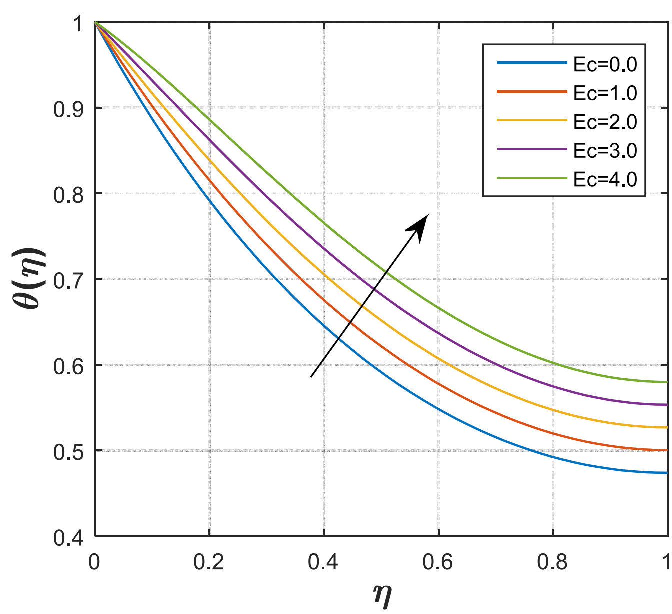

Fig. 9. Profile of temperature for Ec.

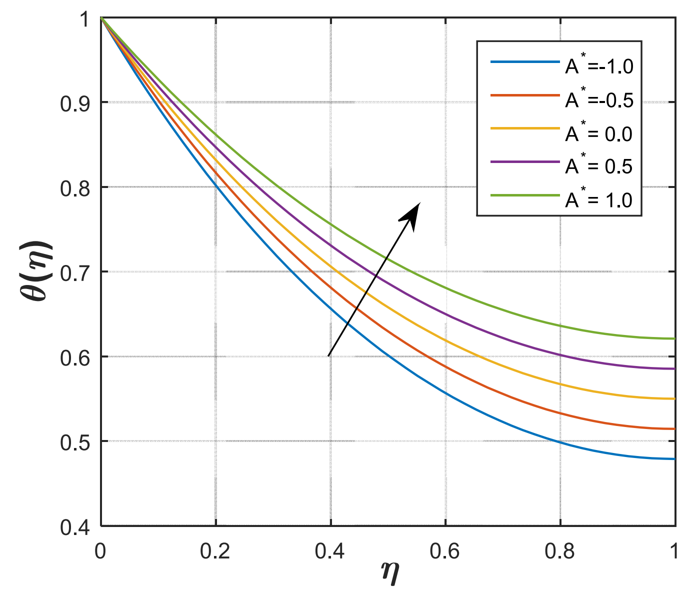

Fig. 10. Profile of temperature for A*.

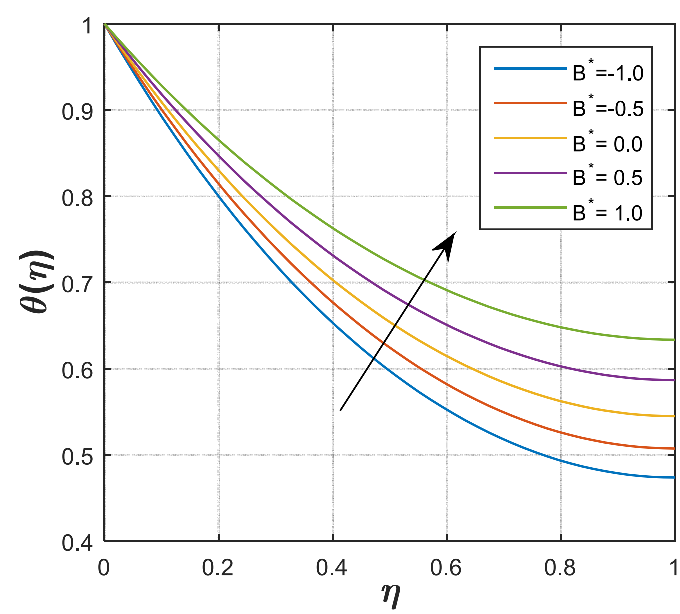

Fig. 11. Profile of temperature for b*.

required, lower values of S would be more effective in maintaining a higher rate of heat transfer.

Fig. 8 describes variation of temperature distribution $\theta(\eta)$ in the boundary layer with Magnetic parameter M in the stretching sheet. An increase in M results in a higher temperature within the boundary layer. This phenomenon occurs because the magnetic field exerts a retarding force on the fluid flow which reduces the fluid velocity. The reduced velocity leads to greater conversion of kinetic energy into thermal energy, causing a rise in the fluid's temperature. This result indicates that the application of a magnetic field can be used as a means to control the thermal behaviour of the fluid, particularly in magnetohydrodynamic (MHD) systems.

Fig. 9 provides a visual representation of variation of temperature distribution $\theta(\eta)$ in the boundary layer with Eckert number Ec in the stretching sheet. As Ec increases, the temperature within the boundary layer also increases. The Eckert number represents the ratio of kinetic energy to enthalpy, and higher values of Ec correspond to greater frictional heating due to viscous dissipation. This additional heat generated by the viscous effects leads to an increase in the overall temperature of the fluid. This behavior is particularly relevant in applications where energy dissipation is significant, as controlling the Eckert number allows for manipulation of the temperature distribution.

Figs. 10 and 11 shows the relationship between variation of temperature profile $\theta(\eta)$ for different values of space dependent heat source/sink parameter A^* and temperature dependent heat source/sink parameter B^*. As both parameters increase, the temperature within the boundary layer rises. This behaviour is due to the fact that both parameters control the internal heat generation within the fluid. Positive values of A^* and B^* correspond to heat generation, which enhances the thermal boundary layer thickness and increases the temperature of the fluid. These findings highlight the role of heat sources and sinks in modifying the temperature field.

5. Conclusion

In this study, we conducted a theoretical analysis of unsteady laminar boundary layer flow and heat transfer over a horizontal sheet in the presence of radiation and non-uniform heat sources or sinks. The findings highlight the significant influence of key parameters.

- An increase in the unsteadiness parameter (S) reduces the velocity profiles and heat flux in the boundary layer. As unsteadiness increases, the flow becomes more synchronized with the stretching surface, decreasing the skin friction coefficient and heat transfer rate.
- Higher Prandtl numbers lead to a reduction in the thermal boundary layer thickness. This causes the temperature distribution to decrease, as fluids with higher Prandtl numbers have lower thermal diffusivity.
- An increase in the radiation parameter enhances the temperature profile within the boundary layer, indicating that radiation plays a significant role in transferring energy and increasing the temperature near the surface.
- The presence of a magnetic field increases the temperature profile. This occurs because the magnetic field reduces fluid velocity, allowing more kinetic energy to be converted into thermal energy, thereby raising the temperature within the boundary layer.
- A higher Eckert number leads to an increase in temperature due to the effect of viscous dissipation. This additional heat generation raises the overall temperature of the fluid in the boundary layer.
- Increasing both the space-dependent (A*) and temperature-dependent (B*) heat sources leads to a higher temperature within the boundary layer. This increase in heat generation thickens the thermal boundary layer and raises the fluid temperature

CRediT authorship contribution statement

Machindranath Diwate: Data curation, Methodology. Jagadish V. Tawade: Supervision, Validation, Visualization. Pradeep G. Janthe: Writing – original draft, Software. Mubariz Garayev: Resources, Formal analysis. Mohammed El-Meligy: Review & editing, Validation. Nitiraj Kulkarni: Conceptualization, Validation. Manish Gupta: Investigation, Visualization. M. Ijaz Khan: Writing – review & editing, Formal analysis.

6. Future scope

Future research in this area can explore the effects of non-Newtonian fluid behaviour, viscoelastic properties, and turbulent flow regimes on boundary layer characteristics in complex geometries, such as curved surfaces and rotating machinery. These studies could enhance the understanding of heat transfer and flow dynamics in advanced applications like polymer processing, biomedical devices, and energy-efficient systems. Additionally, incorporating transient boundary conditions, such as fluctuating heat sources or oscillating surfaces, could provide valuable insights for optimizing design parameters in industries requiring precise thermal control and efficient energy management.

Data availability

The data will be made available on a reasonable request to the corresponding author.

Conflict of interest

The author declares no conflict of interest from this research.

Acknowledgment

The authors extend their appreciation to King Saud University for funding this work through Researchers Supporting Project number (RSPD2024R1056), King Saud University, Riyadh, Saudi Arabia.

Nomenclature

Greek Symbols

Symbol	Description	Units
λ	Dimensionless film thickness	–
μ	Dynamic viscosity	Pa·s
ρ	Fluid density	kg/m^3
σ	Stefan-Boltzmann constant	W/m^2·K^4
η	Similarity variable	–
τ	Shear stress	Pa
$\theta(\eta$	Dimensionless temperature	–

Other Symbols

Symbol	Description	Units
Pr	Prandtl number	–
R	Radiation parameter	–
Ec	Eckert number	–
M	Magnetic parameter	–
A^*	Space-dependent heat source/sink coefficient	–
B^*	Temperature-dependent heat source/sink coefficient	–
S	Unsteadiness parameter	–
$f(\eta)$	Stream function	–
B	Magnetic field strength	T
T	Temperature	K
U	Surface velocity	m/s
q'''	Internal heat generation or absorption	W/m^3
k	Thermal conductivity	W/m·K

(*continued on next page*)

(*continued*)

Symbol	Description	Units
k^*	Absorption coefficient	m^{-1}
Cp	Specific heat capacity	J/kg·K
T_{ref}	Reference temperature	K
q^r	Heat flux	W/m^2
Re_x	Reynolds number	–
C_f	Skin friction coefficient	–
$h(t)$	Boundary layer thickness	m

References

Abel, M. S., Mahesha, N., & Tawade, J. (2009). Heat transfer in a liquid film over an unsteady stretching surface with viscous dissipation in presence of external magnetic field. *Applied Mathematical Modelling, 33*(8), 3430–3441.

Abel, M. S., Tawade, J., & Nandeppanavar, M. M. (2009). Effect of non-uniform heat source on MHD heat transfer in a liquid film over an unsteady stretching sheet. *International Journal of Non-linear Mechanics, 44*(9), 990–998.

Awais, M., & Salahuddin, T. (2023). Natural convection with variable fluid properties of couple stress fluid with Cattaneo-Christov model and enthalpy process. *Heliyon, 9*(8), Article e18546.

Awais, M., & Salahuddin, T. (2024). Variable thermophysical properties of magnetohydrodynamic cross fluid model with effect of energy dissipation and chemical reaction. *International Journal of Modern Physics B, 38*(16), Article 2450197.

Awais, M., Salahuddin, T., & Muhammad, S. (2023). Evaluating the thermo-physical characteristics of non-Newtonian Casson fluid with enthalpy change. *Thermal Science and Engineering Progress, 42*, Article 101948.

Awais, M., Salahuddin, T., & Muhammad, S. (2024). Effects of viscous dissipation and activation energy for the MHD Eyring-powell fluid flow with Darcy-Forchheimer and variable fluid properties. *Ain Shams Engineering Journal, 15*(2), Article 102422.

Bilal, M., Safdar, M., Ahmed, S., & Khan, R. A. (2023). Analytic similarity solutions for fully resolved unsteady laminar boundary layer flow and heat transfer in the presence of radiation. *Heliyon, 9*(4), Article e14765.

Crane, L. J. (1970). Flow past a stretching plate. *Zeitschrift für angewandte Mathematik und Physik ZAMP, 21*, 645–647.

Hamid, A., Chu, Y. M., Khan, M. I., Kumar, R. N., Gowd, R. J. P., & Prasannakumara, B. C. (2021). Critical values in axisymmetric flow of magneto-cross nanomaterial towards a radially shrinking disk. *International Journal of Modern Physics B, 35*, Article 2150105.

Kazemi, M., Salehpour, S. Y., Shahbaazy, F., Behzadpoor, S., Pirouzi, S., & Jafarpour, S. (2022). Participation of energy storage-based flexible hubs in day-ahead reserve regulation and energy markets based on a coordinated energy management strategy. *International Transactions on Electrical Energy Systems, 2022*(1), Article 6481531.

Khalafian, F., Iliaee, N., Diakina, E., Parsa, P., Alhaider, M. M., Masali, M. H., … Zhu, M. (2024). Capabilities of compressed air energy storage in the economic design of renewable off-grid system to supply electricity and heat costumers and smart charging-based electric vehicles. *Journal of Energy Storage, 78*, Article 109888.

Li, Y. X., Al-Khaled, K., Khan, S. U., Sun, T. C., Khan, M. I., & Malik, M. Y. (2021). Bio-convective Darcy-Forchheimer periodically accelerated flow of non-Newtonian nanofluid with Cattaneo–Christov and Prandtl effective approach. *Case Studies in Thermal Engineering, 26*, Article 101102.

Liang, H., & Pirouzi, S. (2024). Energy management system based on economic Flexi-reliable operation for the smart distribution network including integrated energy system of hydrogen storage and renewable sources. *Energy, 293*, Article 130745.

Muhammad, K., Nisar, Z., Alhuthali, A., & Hussien, M. (2024). Statistical and numerical analysis of electrically conducting hybrid nanomaterial near the stagnation region. *Journal of Thermal Analysis and Calorimetry*, 1–10.

Nasir, S., & Berrouk, A. S. (2024). Comparative study of computational frameworks for magnetite and carbon nanotube-based nanofluids in enclosure. *Journal of Thermal Analysis and Calorimetry, 149*(5), 2403–2423.

Nasir, S., Berrouk, A. S., & Aamir, A. (2024). Efficiency analysis of solar radiation on chemical radioactive nanofluid flow over a porous surface with magnetic field. *Case Studies in Thermal Engineering*, Article 105231.

Nasir, S., Berrouk, A. S., Gul, T., & Zari, I. (2023). Chemically radioactive unsteady nonlinear convective couple stress Casson hybrid nanofluid flow over a gyrating sphere. *Journal of Thermal Analysis and Calorimetry, 148*(22), 12583–12595.

Nasir, S., Berrouk, A. S., Tassaddiq, A., Aamir, A., Akkurt, N., & Gul, T. (2023). Impact of entropy analysis and radiation on transportation of MHD advance nanofluid in porous surface using Darcy-Forchheimer model. *Chemical Physics Letters, 811*, Article 140221.

Nasir, S., Sirisubtawee, S., Juntharee, P., Berrouk, A. S., Mukhtar, S., & Gul, T. (2022). Heat transport study of ternary hybrid nanofluid flow under magnetic dipole together with nonlinear thermal radiation. *Applied Nanoscience, 12*(9), 2777–2788.

Norouzi, M., Aghaei, J., Niknam, T., Pirouzi, S., & Lehtonen, M. (2022). Bi-level fuzzy stochastic-robust model for flexibility valorizing of renewable networked microgrids. *Sustainable Energy, Grids and Networks, 31*, Article 100684.

Norouzi, M., Aghaei, J., Pirouzi, S., Niknam, T., & Fotuhi-Firuzabad, M. (2022). Flexibility pricing of integrated unit of electric spring and EVs parking in microgrids. *Energy, 239*, Article 122080.

Pirouzi, S. (2023). Network-constrained unit commitment-based virtual power plant model in the day-ahead market according to energy management strategy. *IET Generation, Transmission & Distribution, 17*(22), 4958–4974.

Qian, W. M., Khan, M. I., Shah, F., Khan, M., Chu, Y. M., Khan, W. A., & Nazeer, M. (2022). Mathematical modeling and MHD flow of micropolar fluid toward an exponential curved surface: Heat analysis via ohmic heating and heat source/sink. *Arabian Journal for Science and Engineering, 47*(2022), 867–878.

Sakiadis, B. C. (1961). Boundary-layer behavior on continuous solid surfaces: I. Boundary-layer equations for two-dimensional and axisymmetric flow. *AIChE Journal, 7*(1), 26–28.

Salahuddin, T. (2023). *Numerical techniques in MATLAB: Fundamental to advanced concepts*. CRC Press.

Salahuddin, T., & Awais, M. (2023). Cattaneo-christov flow analysis of unsteady couple stress fluid with variable fluid properties: By using adam's method. *Alexandria Engineering Journal, 81*, 64–86.

Salahuddin, T., Awais, M., Khan, M., & Altanji, M. (2021). Analysis of transport phenomenon in cross fluid using Cattaneo-Christov theory for heat and mass fluxes with variable viscosity. *International Communications in Heat and Mass Transfer, 129*, Article 105664.

Salahuddin, T., Awais, M., & Xia, W. F. (2021). Variable thermo-physical characteristics of Carreau fluid flow by means of stretchable paraboloid surface with activation energy and heat generation. *Case Studies in Thermal Engineering, 25*, Article 100971.

Salahuddin, T., Iqbal, M. A., Bano, A., Awais, M., & Muhammad, S. (2023). Cattaneo-Christov heat and mass transmission of dissipated Williamson fluid with double stratification. *Alexandria Engineering Journal, 80*, 553–558.

Sarfraz, M., & Khan, M. (2022). Significance of ethylene glycol-based CNT Homann nanofluid flow over a biaxially stretching surface. *Waves in Random and Complex Media*, 1–15.

Sarfraz, M., & Khan, M. (2024). Rheology of gyrotactic microorganisms in jeffrey fluid flow: A stability analysis. *Modern Physics Letters B, 38*(5), Article 2450003.

Sarfraz, M., Yasir, M., & Khan, M. (2023). Multiple solutions for non-linear radiative mixed convective hybrid nanofluid flow over an exponentially shrinking surface. *Scientific Reports, 13*(1), 3443.

Sikiadis, B. C. (1961). Boundary-Layer behavior on continuous solid surfaces. *AIChE Journal, 7*, 26–28.

Sulochana, G., Prasad, C. V., Bhatti, S. K., Madhav, V. V. V., Saxena, K. K., Khan, M. I., … Khan, M. I. (2024). Impact of multi-walled carbon nanotubes (MWCNTs) on hybrid biodiesel blends for cleaner combustion in CI engines. *Energy, 303*(2024), 131911.

Teja, D. V. H., Muvvala, P., Nittala, N. A. P., Bandhu, D., Khan, M. I., Saxena, K. K., & Khan, M. I. (2024). Comparative performance analysis of recuperative helium and supercritical CO_2 brayton cycles for high-temperature energy systems. *Energy, 312*, 133469.

Tsai, R., Huang, K. H., & Huang, J. S. (2008). Flow and heat transfer over an unsteady stretching surface with non-uniform heat source. *International Communications in Heat and Mass Transfer, 35*(10), 1340–1343.

Wang, C. (2006). Analytic solutions for a liquid film on an unsteady stretching surface. *Heat and Mass Transfer, 42*, 759–766.

Zhang, X., Yu, X., Ye, X., & Pirouzi, S. (2023). Economic energy managementof networked flexi-renewable energy hubs according to uncertainty modeling by the unscented transformation method. *Energy, 278*, Article 128054.

Zhao, T. H., Khan, M. I., Qayyum, S., Kumar, R. N., Chu, Y. M., & Prasannakumara, B. C. (2021). Comparative study of ferromagnetic hybrid (manganese zinc ferrite, nickle zinc ferrite) nanofluids with velocity slip and convective conditions. *Physica Scripta, 96*, Article 075203.